



Seismic retrofit of asymmetric structures using steel plate slit dampers



Jinkoo Kim *, Jaeyoung Jeong

Dept. of Civil and Architectural Engineering, Sungkyunkwan University, Chunchun-Dong, Jangan-Gu, Suwon 440-749, Republic of Korea

ARTICLE INFO

Article history:

Received 17 November 2015

Received in revised form 4 February 2016

Accepted 5 February 2016

Available online xxxx

Keywords:

Asymmetric structures

Steel plate slit dampers

Seismic retrofit

Ductility demand

ABSTRACT

A seismic design and retrofit procedure were developed for estimating the proper amount of steel plate slit dampers required to keep the seismic response of low-rise asymmetric structures within a given target performance level. Parametric studies for displacement response of a single story plan-wise asymmetric structure were conducted with varying eccentricities between center of mass and center of stiffness. Then a procedure was developed to distribute the damper based on the ductility demand of the structure. The procedure was applied to install slit dampers at proper locations of low-rise structures with horizontal and/or vertical irregularities subjected to an earthquake load. According to the nonlinear static and dynamic analysis results, the structure with hysteretic dampers installed in accordance with the proposed procedure showed satisfactory inter-story drifts in both the stiff and the flexible edges when they were subjected to the design level seismic load.

© 2015 Elsevier Ltd. All rights reserved.

1. Introduction

It has been reported that asymmetric structures are especially vulnerable to earthquake-induced damage. According to the ASCE 7-13 [1], torsional irregularity is defined to exist where the maximum story drift at one end of the structure transverse to an axis is more than 1.2 times the average of the story drifts at the two ends of the structure. Many researchers have investigated the seismic response mitigation of asymmetric buildings using supplemental energy dissipation devices. Goel [2] studied the effects of supplemental viscous damping on seismic response of one-way asymmetric system and found that edge deformations in asymmetric systems could be reduced by proper selection of supplemental damping parameters. Kim and Bang [3] proposed a strategy based on modal analysis for an appropriate plan-wise distribution of viscoelastic dampers to minimize the torsional responses of an asymmetric structure with one axis of symmetry subjected to an earthquake-induced dynamic motion. They also found that the viscoelastic dampers were more effective than viscous dampers in controlling the torsional response of a plan-wise asymmetric building structure. Lin and Chopra [4] investigated the effectiveness of viscous dampers for elastic single story asymmetric system, and showed that the reduction in the seismic response achieved by a judiciously selected asymmetric distribution of viscous dampers can be significantly larger compared to symmetric distribution. De La Llera et al. [5] carried out analytical and experimental research of linear asymmetric structures with frictional and viscoelastic dampers, and showed that the energy dissipation devices prove useful in controlling the uneven deformation demand occurring in structural members of torsionally unbalanced structures. Petti and De

Iulii [6] proposed a method to optimally locate the viscous dampers for torsional response control in asymmetric plan systems by using modal analysis techniques. It was found that optimal damping eccentricity moves from the flexible edge to the mass center by reducing the structural eccentricity. Mevada and Jangid [7] investigated the seismic response of linearly elastic, single-story, one-way asymmetric building with linear and non-linear viscous dampers. It was shown that the non-linear viscous dampers were quite effective in reducing the responses and the damper force depends on system asymmetry and supplemental damping. Khante and Nirwan [8] applied a tuned mass damper for mitigation of torsional effect in an asymmetric structure subjected to seismic load, and investigated the optimum parameters for TMD with respect to the design variables such as eccentricity ratios, uncoupled torsional to lateral frequency ratios, mass ratios etc. Bharti et al. [9] investigated the seismic behavior of an asymmetric plan building with MR (Magnetorheological) dampers, and found that MR damper-based control systems are effective for plan asymmetric systems. They also investigated the influence of the building parameters and damper command voltage on the control performance through a parametric study. Almazana et al. [10] studied the response of asymmetrical linear and nonlinear structures subjected to unidirectional and bidirectional seismic excitations, equipped with one or two Tuned Mass Dampers (TMDs), and obtained the optimized parameters of each TMD by applying the concept of general torsional balance.

Most of the previous studies on mitigation of asymmetric behavior using energy dissipation devices were focused on elastic behavior of structures [2–9]. Paulay [11] suggested a rational design philosophy for performance-based seismic design of asymmetric structures subjected to inelastic deformation. He recommended a design procedure in which the ductility demand in each structural element does not exceed a given limit state. The same approach was applied in this study for application

* Corresponding author.

E-mail address: jkim12@skku.edu (J. Kim).

of steel plate slit dampers to mitigate torsional effect as well as overall responses. Parametric studies for displacement response of a single story plan-wise asymmetric structure were conducted with the eccentricity ratio as a main parameter. Then a systematic and practical design procedure was developed to distribute the steel damper based on the ductility demand of the structure. The procedure was applied to install proper amount of steel plate slit dampers at stiff and flexible edges of low-rise structures with horizontal and vertical irregularities to reduce torsional effect as well as overall seismic responses.

2. Seismic retrofit design procedure for a plan asymmetric structure

2.1. Ductility demand in a single-story asymmetric structure

Fig. 1 shows an idealized one-story structural plan with lateral stiffness eccentricity along the x axis. The floor is considered as rigid diaphragm, and the model structure belongs to a torsionally rigid system. When lateral force of V is applied to the center of mass, CM, along the y axis, torsional moment M_t is generated due to the eccentricity between CM and the center of rigidity, CR, and the force at each vertical element contributed from the direct shear and the torsional moment can be obtained as follows [11]

$$V_{iy} = \left(\frac{k_{iy}}{\sum k_{iy}} \right) V_y + y_i k_{iy} \frac{M_t}{K_t} \tag{1}$$

where the torsional stiffness K_t is expressed as follows

$$K_t = \sum y_i^2 k_{ix} + \sum x_i^2 k_{iy} \tag{2}$$

where x_i and y_i are the distances from CR to *i*th element, k_{xi} and k_{yi} are the element lateral stiffness for x and y axes, respectively, expressed in the form

$$k_i = \frac{V_i}{\Delta_i} \tag{3}$$

where V_i is the applied load to the *i*th element and Δ_i is the resulting deflection. The maximum displacement at CM, Δ_m , is obtained by summation of the displacement due to lateral load, Δ'_m , and torsion, Δ''_m , as follows

$$\Delta_m = \Delta'_m + \Delta''_m = \frac{V}{\sum k_i} + \theta_t e_r \tag{4}$$

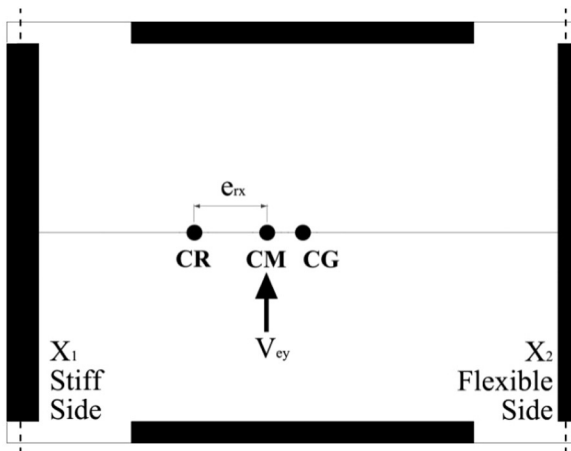


Fig. 1. Structural plan of an idealized asymmetric structure.

where e_r is the structural eccentricity between CM and CR of the system. The rotation angle, θ_t , and the maximum displacement at CM can be obtained as follows

$$\theta_t = M_t K_t = e_r \frac{V}{K_t} \tag{5}$$

$$\Delta_m = V \left[1 / \sum k_i + e_r^2 / K_t \right] \tag{6}$$

The yield displacements of each element and at CM along the y axis are obtained by Eqs. (7a) and (7b), respectively:

$$\Delta_{yi} = \frac{V_{yi}}{k_i} \quad \Delta_y = \frac{\sum V_{iy}}{\sum k_i} \tag{7a, b}$$

where V_{yi} is the yield force of the *i*th element. The post-yield displacement, Δ_u , of the system at CM is obtained as follows:

$$\Delta_u = (\mu_\Delta - 1) \Delta_y \tag{8}$$

where μ_Δ is the ductility demand at CM. When all structural elements are designed to have similar demand to strength ratio for design load, all members start to yield almost at the same time when the load reaches a yield level. In this case the element with largest stiffness will show the smallest yield displacement. If post-yield stiffness is zero, the torsional moment and the twisting angle at yield no longer increase until collapse. After yielding of the system lateral displacements of all elements increase without rotation and the post-yield displacements of all elements are the same. In this case the element with largest stiffness will have the largest ductility demand. In a structure with post-yield stiffness the torsional deformation and the twisting angle change after yielding. When a seismic story force V_E , higher than the yield force V_y , is acting on the structure, the post-yield rotation angle θ_{tu} can be obtained as follows considering the post-yield stiffness of the structure along y axis, a :

$$\theta_{tu} = e_r \frac{V_y}{K_t} + e_r \frac{(V_E - V_y)}{K_{tu}} \tag{9}$$

$$K_{tu} = \sum y_i^2 k_{xi} + \alpha \sum x_i^2 k_{yi} \tag{10}$$

In Fig. 1 the maximum displacements at the stiff edge, Δ_{u1} , and at the flexible edge, Δ_{u2} , are obtained as follows:

$$\begin{aligned} \Delta_{u1} &= \Delta_y + (\mu_\Delta - 1) \Delta_y - x_1 \theta_{tu} \\ \Delta_{u2} &= \Delta_y + (\mu_\Delta - 1) \Delta_y + x_2 \theta_{tu} \end{aligned} \tag{11a, b}$$

According to Paulay [11], the primary aim of the design strategy for asymmetric structure should be to ensure that the expected displacement demand on the system does not exceed the displacement ductility capacity of elements. In this reasoning the ductility demand at each side, obtained as follows, should be less than or equal to the given ductility limit state, μ_L :

$$\mu_1 = \frac{\Delta_{u1}}{\Delta_{y1}} = \mu_\Delta \frac{\Delta_y}{\Delta_{y1}} - x_1 \frac{\theta_{tu}}{\Delta_{y1}} \leq \mu_L \tag{12a}$$

$$\mu_2 = \frac{\Delta_{u2}}{\Delta_{y2}} = \mu_\Delta \frac{\Delta_y}{\Delta_{y2}} - x_2 \frac{\theta_{tu}}{\Delta_{y2}} \leq \mu_L \tag{12b}$$

where μ_Δ is the ductility demand at CM.

2.2. Required damping for seismic retrofit

In this section a simple design procedure was proposed to estimate the required added damping for seismic retrofit of an asymmetric

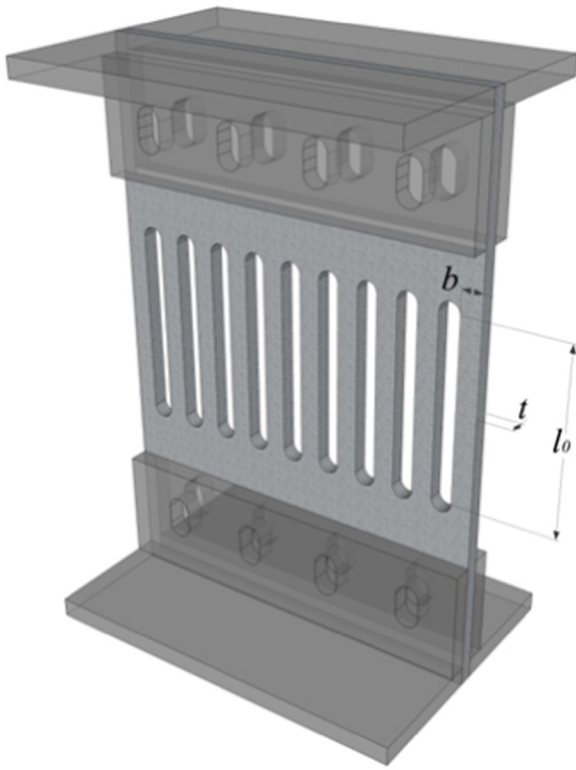


Fig. 2. Configuration of a typical steel plate slit damper.

structure. The retrofit design procedure was developed to satisfy the condition that the ductility demands of ground motions at both stiff and flexible edges satisfy a given limit state when the structure is subjected to design level earthquake load. The equivalent damping of a structure subjected to inelastic deformation with ductility demand of μ can be expressed as follows [12]:

$$\zeta_{eq} = \frac{2(\mu-1)(1-\alpha)}{\pi\mu(1+\alpha\mu-\alpha)} \quad (13)$$

where α is the post-yield stiffness of the original system. The ductility demand can be computed by either a static method such as the capacity spectrum method or a dynamic time history analysis using the ground motion scaled to meet the design spectrum. Using the above relationship between equivalent damping and ductility ratio, the equivalent damping to be added to satisfy the given limit ductility ratio is computed as follows:

$$\zeta_d = \frac{2(\mu_\Delta-1)(1-\alpha)}{\pi\mu_\Delta(1+\alpha\mu_\Delta-\alpha)} - \frac{2(\mu_L-1)(1-\alpha)}{\pi\mu_L(1+\alpha\mu_L-\alpha)} - \zeta_i \quad (14)$$

where μ_Δ is the ductility demand at CM at the performance point, μ_L is the given ductility limit state, and ζ_i is the inherent damping ratio of a structure which was assumed to be 5% of the critical damping. The first and the second terms on the right-hand-side of Eq. (14) correspond to the effective damping at the performance point and at the target deformation, respectively. The difference between the two effective damping ratios minus the inherent damping is the damping ratio to be provided by the added dampers to satisfy the target ductility demand. Once the total required damping is obtained, it is distributed to each story based on the story ductility demand. The amount of damping allocated to the i th story, ζ_{di} , is divided into the stiff side, ζ_{dis} , and the flexible side, ζ_{dif} , based on their relative ductility demands as follows:

$$\zeta_{dis} = \frac{\mu_1}{\mu_1 + \mu_2} \zeta_{di}; \quad \zeta_{dif} = \frac{\mu_2}{\mu_1 + \mu_2} \zeta_{di}. \quad (15)$$

In this study the target ductility demand was set to be 3.0 based on the recommendation of the SEOAC Bluebook [13].

2.3. Estimation of the required strength of slit dampers

Once the required damping ratios at stiff and flexible sides at each story are obtained based on their relative ductility demands, the required yield strengths of the steel plate slit dampers at stiff and flexible sides are determined from the relationship between the given required effective damping and the work done by the dampers using the formula provided

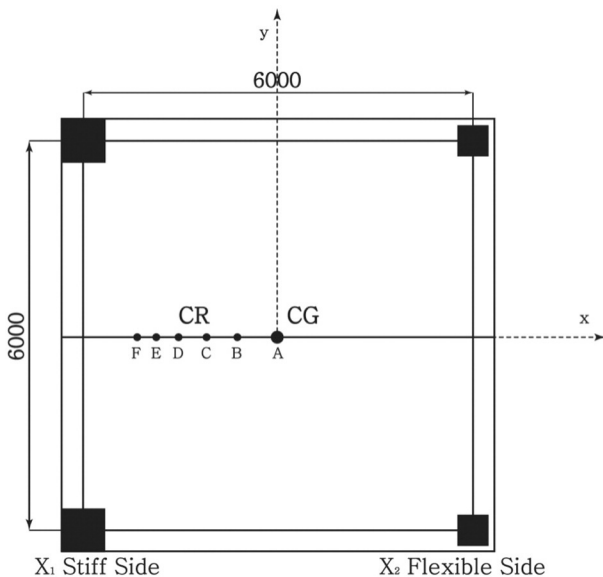


Fig. 3. Locations of the center of rigidity in the single-story analysis model structures (unit: mm).

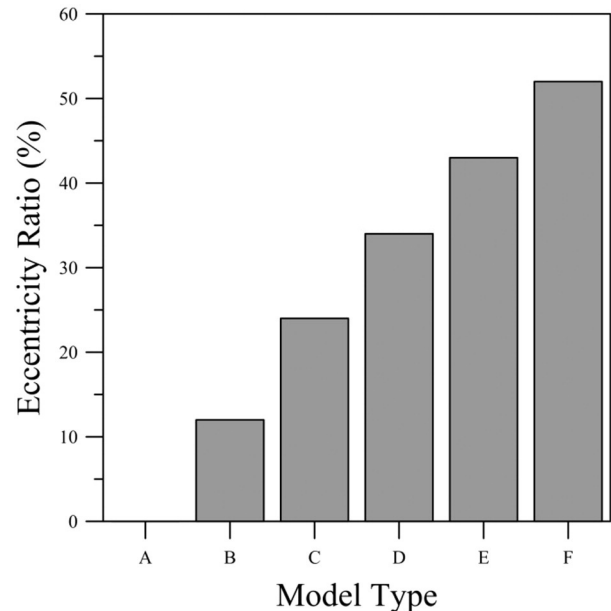


Fig. 4. Eccentricity ratios of single-story model structures.

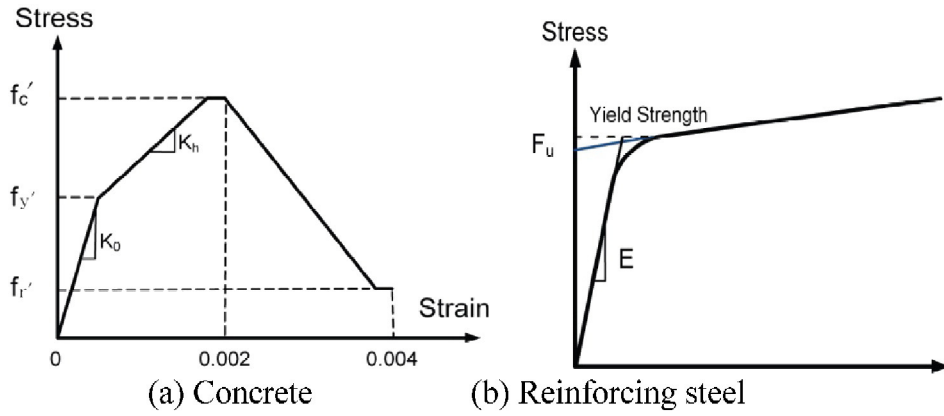


Fig. 5. Nonlinear models for reinforced concrete.

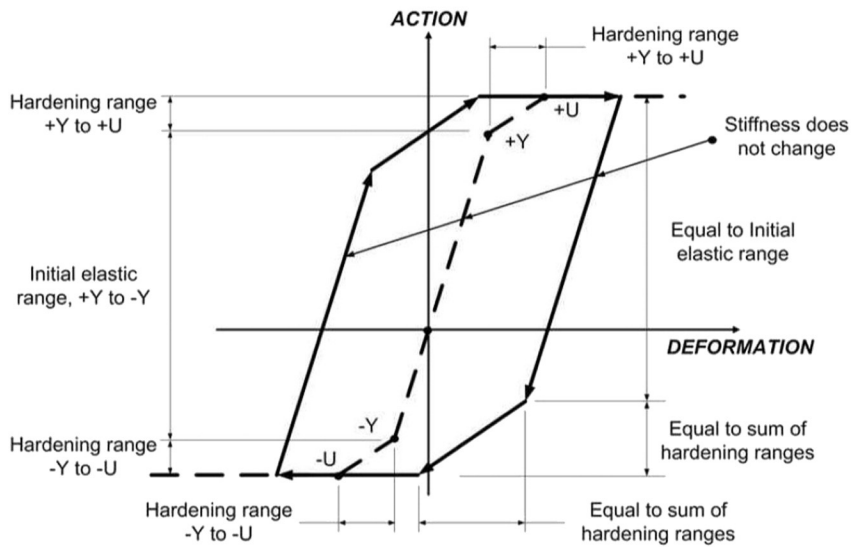
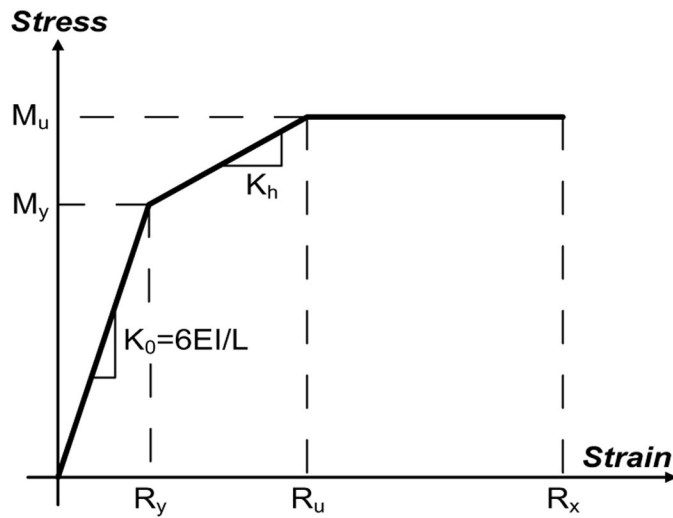


Fig. 6. Idealized nonlinear force–deformation relationship of columns.

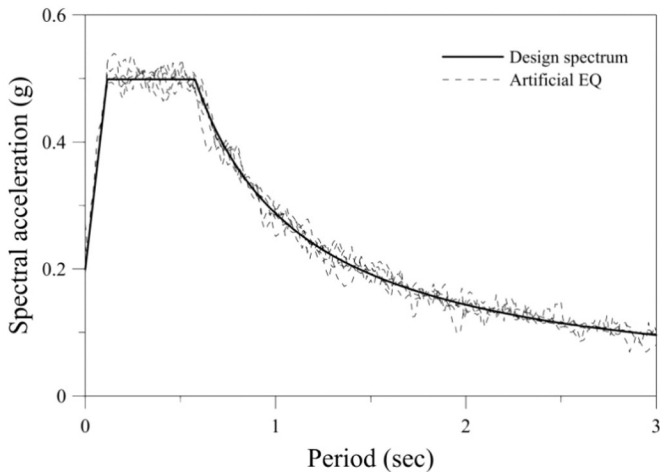


Fig. 7. Response spectra of the seven artificial ground motions generated based on the design spectrum.

by ASCE 41-13 [14] for displacement dependent energy dissipation devices as follows:

$$\zeta_{di} = \frac{\sum_j W_j}{4\pi W_k} \quad (16)$$

where W_j is the work done by the j th slit damper in 1 cycle of vibration obtained using the yield force of the device (initially unknown) and the given inter-story drift, and W_k is the maximum strain energy in the structure. The summation extends over all devices. For evaluation of the work done by the dampers and the maximum strain energy in the structure, the force–displacement relationship of the slit dampers was assumed to be elastic–perfectly plastic. Even though not explicitly considered, the target inter-story drift was set to be 1.5% of the story height which corresponds to the allowable story drift of structures belonging to the risk category IV specified in the ASCE 7-13 [1].

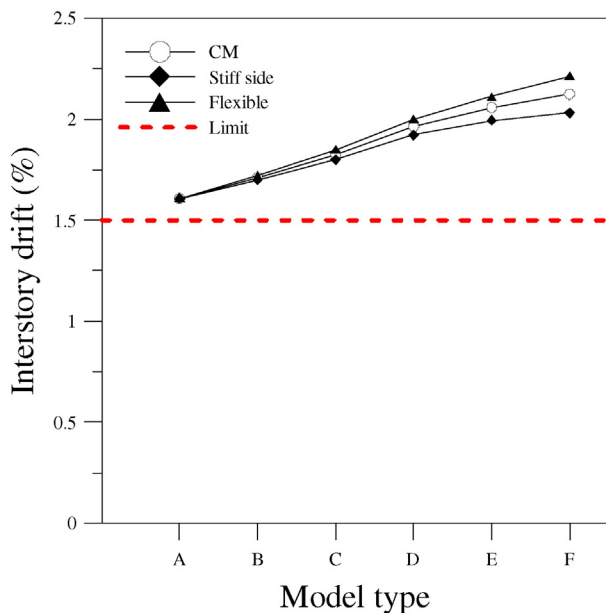


Fig. 8. Mean story drift of the single story structures obtained from nonlinear time history analyses using seven artificial ground motions.

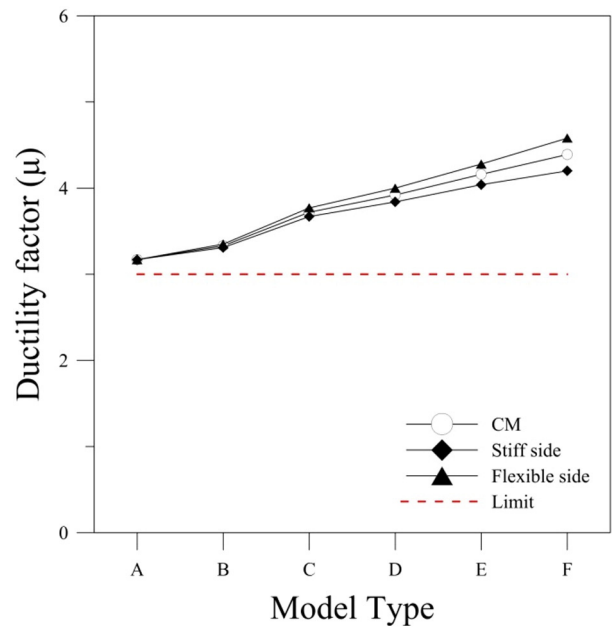


Fig. 9. Mean ductility demands of the single story structures obtained from nonlinear time history analyses.

3. Strength of steel plate slit dampers

The steel plate slit damper considered in this study is composed of many vertical strips as shown in Fig. 2. The in-plane stiffness of the slit damper subjected to horizontal shear force can be obtained as follows based on the assumption that the ends of the narrow strips are fully restrained from rotation:

$$k_d = n \frac{12EI}{l_o^3} = n \frac{Etb^3}{l_o^3} \quad (17)$$

where n = number of strips, t = thickness of strips, b = width of strips, and l_o = length of the vertical strip. Chan and Albermani [15] derived

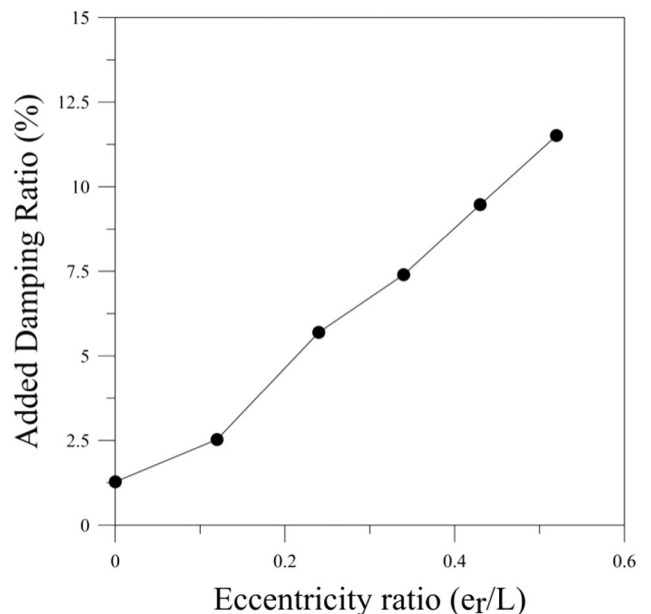


Fig. 10. Required damping ratio for seismic retrofit in the single story model structures.

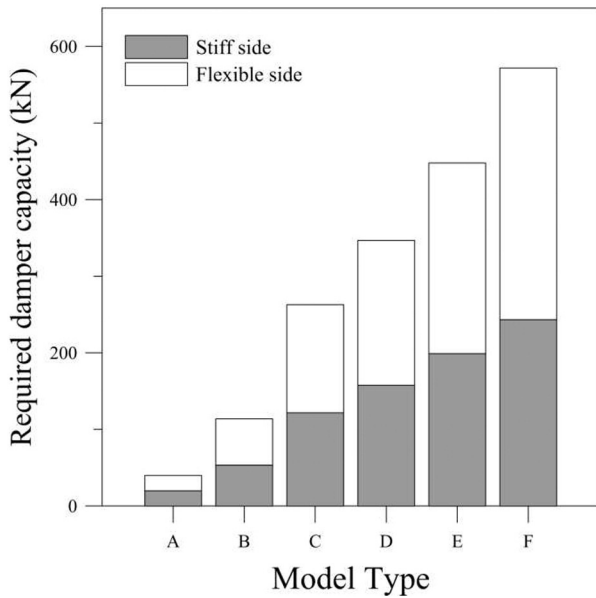


Fig. 11. Required yield strength of slit dampers for seismic retrofit.

the yield strength of a slit damper assuming elastic–perfectly-plastic behavior, which is summarized as follows. When displacement is large, plastic hinges form at both ends of the strip with the full plastic moment M_p obtained by multiplication of the yield stress and the plastic section modulus:

$$M_p = \sigma_y \frac{tb^2}{4}. \tag{18}$$

From the equivalence of the internal work, $P_y \delta_p$, and the external work, $2nM_p \theta_p$, where δ_p is the plastic displacement, and $l_0 \theta_p$, and θ_p are the plastic rotation, the yield force of the slit damper, P_y , can be obtained as follows:

$$P_y = F_{y.slit} = \frac{2nM_p}{l_0} = \frac{n \sigma_y tb^2}{2l_0} \tag{19}$$

In this study the slit dampers are made of structural steel with a yield stress of 325 MPa and the thickness of the strip t is 20 mm, while the length of the slit l_0 , the width of the strip b , and the number of strip n are changed to produce the desired yield force. The force–displacement relationship of the slit damper was assumed to be bilinear with elastic–perfectly plastic behavior.

Table 1
Yield strength of the slit dampers used for seismic retrofit of the single-story structure.

Model	Side	P_y (kN)
A	Stiff	20
	Flexible	20
B	Stiff	53.5
	Flexible	60.4
C	Stiff	121.7
	Flexible	141.2
D	Stiff	157.7
	Flexible	189.2
E	Stiff	199.1
	Flexible	248.8
F	Stiff	243.4
	Flexible	328.6

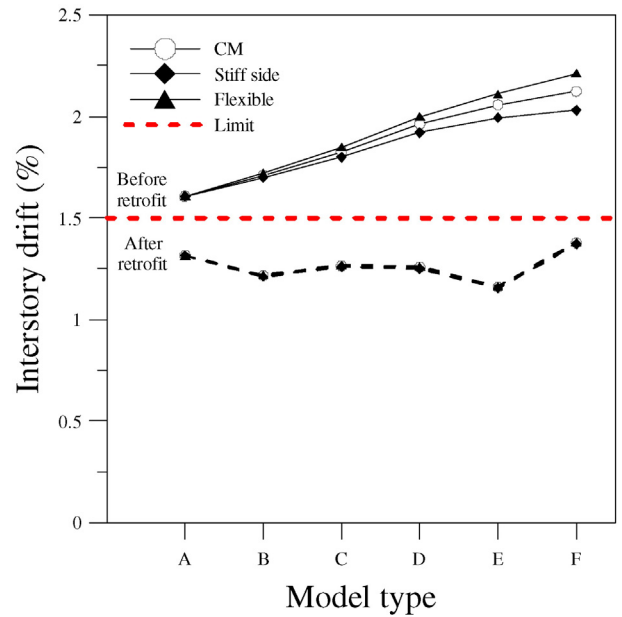


Fig. 12. Mean interstory drifts of model structures obtained from time history analyses using seven earthquake records.

4. Seismic retrofit of single story shear buildings with plan asymmetry

4.1. Design and seismic performance of model structures

For the parametric study an idealized one-story building consisting of a rigid slab supported on four RC columns shown in Fig. 3 was used. The structure has a 6 m span length and 3 m height. The columns were designed to resist the dead and live loads of 6.6 kN/m² and 1.0 kN/m², respectively. The model structure was designed in such a way that eccentricity exists only along the x axis, and the seismic load acts at the center of mass, CM, along the y axis. The mass was estimated from the mass of the floor slab and the mass of the columns. The mass of the slab is assumed to be uniformly distributed so that CM coincides

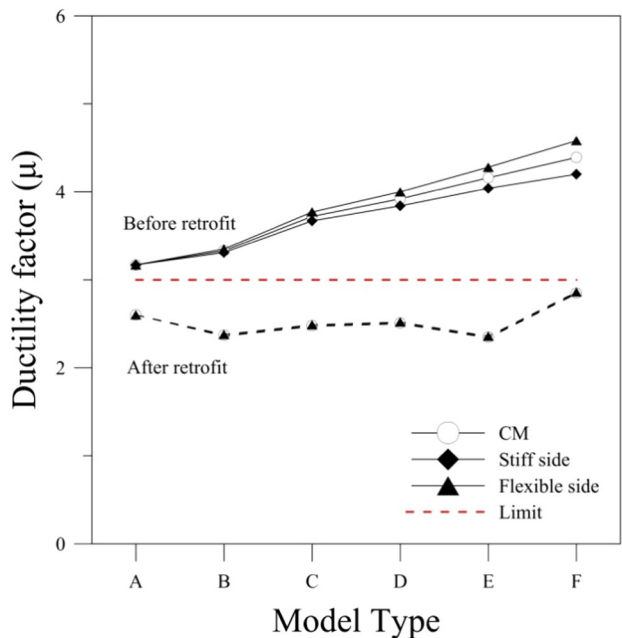


Fig. 13. Mean ductility demands of model structures obtained from time history analyses using seven artificial earthquake records.

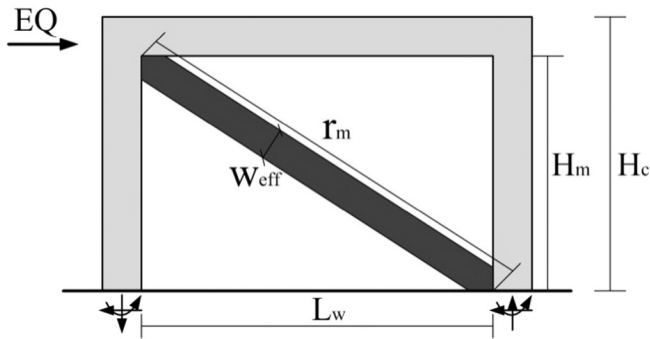


Fig. 14. Equivalent strut idealization of a masonry wall.

with the center of geometry (CG) when there is no eccentricity. The fundamental natural period of the system is 0.11 s, and the uncoupled torsional to lateral frequency ratio is 1.6. For the parametric study six different analysis models were prepared with the stiffness eccentricity with respect to the CM varied from 0 to 50% of the half dimension of the slab which is 300 cm. The stiffness asymmetry was produced by decreasing the size of the columns in the flexible edge and increasing the size of columns in the stiff edge while the total bending stiffness of columns remained the same. The column size of the symmetric structure is 40 × 40 cm on both sides, and those of the structure with 50% eccentricity is 30 × 30 cm on the flexible side and 45.6 × 45.6 cm on the stiff side. Fig. 4 shows the eccentricity ratios of the single-story analysis model structures used in the parametric study. The structures have three degrees of freedom, two lateral and one rotational, and only the lateral displacement along the y-axis (transverse direction) was considered in the analysis.

Nonlinear static and dynamic analyses were carried out using the program code Perform 3-D [16]. The stress–strain material model of Paulay and Priestley [17] was used for concrete as shown in Fig. 5(a), in which the ultimate and yield strengths of concrete, f_c and f_y , are 21 MPa and 12 MPa (cylinder strength), respectively, and the residual strength, f_r , is defined as 20% of the ultimate strength. The strain at the ultimate strength is 0.002, and the ultimate strain is defined as 0.004. The reinforcing steel was modeled with bi-linear lines with the ultimate strength of 400 MPa as shown in Fig. 5(b). The chord rotation type nonlinear behavior model for columns specified in the ASCE/SEI 41-13 [18] and shown in Fig. 6 was used in the analysis. The post-yield stiffness was assumed to be 10% of the initial stiffness. In the nonlinear analysis the

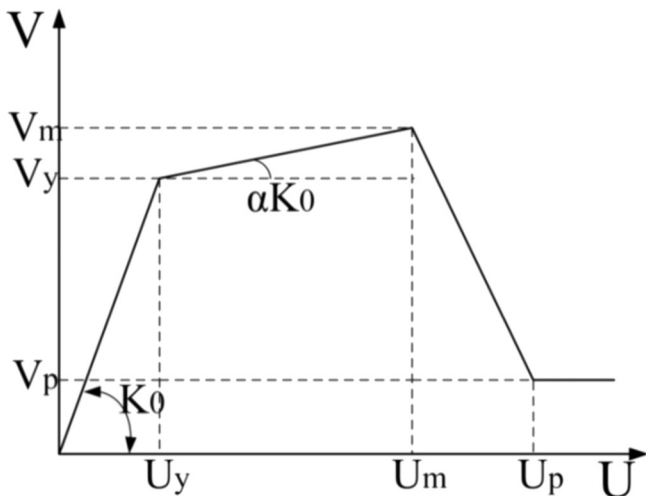


Fig. 15. Idealized nonlinear behavior of a masonry infill panel.

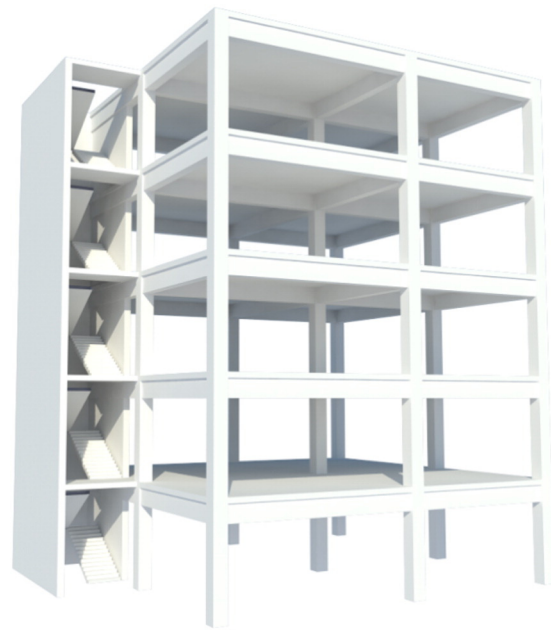


Fig. 16. Perspective view of the 5-story model structure with plan eccentricity.

overstrength factors of 1.5 and 1.25 were applied for concrete and reinforcing bars, respectively. The shear walls were modeled using the Shear Wall fiber elements provided in the Perform 3D. For nonlinear dynamic analyses, seven artificial earthquake records were generated based on the design spectrum using the software EQMAKER [19]. The design spectrum specified in the ASCE 7-13 [1] was constructed using the seismic ground acceleration coefficients, S_{DS} and S_{D1} , of 0.49 and 0.28, respectively. The input parameters to be used for generation of the ground motions are: the seismic acceleration coefficients used, range of period (0.01–3 s.), time step (0.01 s.), and duration of motions (25 s.). Fig. 7 shows the response spectra of the artificial ground motions and the design spectrum.

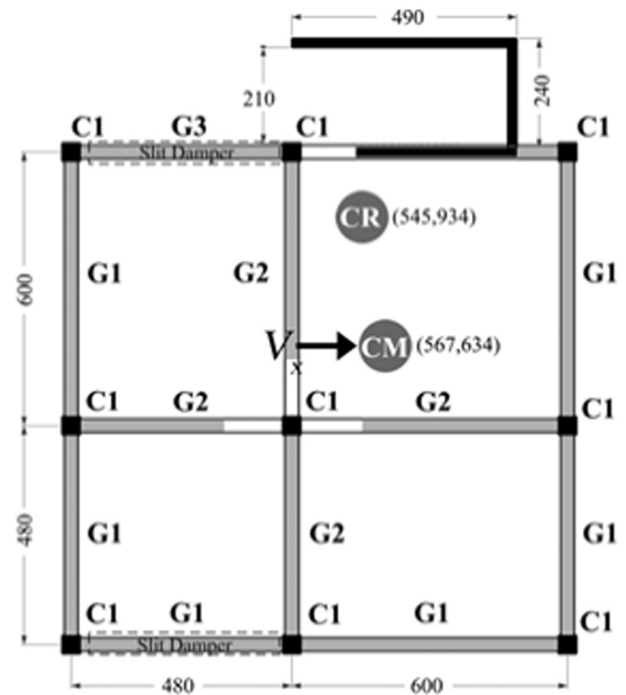


Fig. 17. Structural plan of the 5-story model structure with plan eccentricity (unit: cm).

Table 2
Dimensions of masonry walls in the 5-story model structure with plan eccentricity.

	H_c (m)	H_m (cm)	L_m (cm)	r_m (cm)	θ (degree)	W_{eff} (cm)
MW1	290	240	440	501	30.6	46.7
MW2			560	609	23.2	58.1

Fig. 8 depicts the mean story drifts of the single story structures at CM, stiff side, and flexible side along the y-direction obtained from nonlinear time history analyses using seven artificial ground motions. It can be observed that the mean maximum displacements of all model structures exceed 1.5% of the story height. As expected the displacements of the flexible sides are larger than those of the CM and stiff sides, and the displacements increase as the eccentricity increases. Fig. 9 shows the mean ductility demands obtained by dividing the maximum displacements obtained from time history analyses with the yield displacements. It can be observed that in the structure without eccentricity (Type A) the mean maximum ductility demand is slightly higher than 3.0, while it is around 4.5 in the Type F structure with the largest eccentricity.

4.2. Seismic retrofit of model structures using steel plate slit dampers

In this section the required yield strength of slit dampers was estimated to reduce the seismic response of model structures in such a way that the maximum ductility demand at the center of mass becomes less than the given target value of 3.0 when it is subjected to the design seismic load. The difference between the effective damping corresponding to the maximum ductility demanded by design level seismic load and the effective damping for the target ductility minus the inherent damping was considered as the added damping to be provided by the slit dampers. The mean maximum ductility demands of the model structures with various eccentricities were obtained from the seismic performance evaluations carried out in the previous section. Once the required damping at CM was obtained, it was divided into stiff and flexible sides based on their relative ductility demands. Then the required yield strength of slit dampers was determined from the relationship between the known required effective damping and the work done by the steel plate slit dampers.

Fig. 10 shows the required damping ratios at CM of the single-story analysis model structures with various eccentricities obtained using Eq. (14), where L represents the half length of the span. It can be observed that as the eccentricity ratio increased the required added damping also increased. Fig. 11 depicts the required slit damper capacity at both stiff and flexible sides computed using Eq. (15). The exact yield strengths of slit dampers assigned to the model structures are presented in Table 1. As expected, slit dampers with larger capacity were allocated to flexible sides to minimize the effect of eccentricity. To confirm the validity of the proposed method, nonlinear dynamic analyses were carried out using the seven artificial earthquake records and the mean maximum displacements are plotted in Fig. 12. For comparison the analysis results of the structures before retrofit were also plotted. The analysis results show that, after retrofit with the slit dampers designed and distributed using the proposed method, the mean maximum displacements at the three points are reduced below 1.5% of the story height. It also can be observed that the displacements at CM and at both sides are quite similar to each other. The mean

Table 3
Parameters for nonlinear model of the masonry walls in the 5-story model structure.

	K_0 (10^5) (kN/cm)	V_p (kN)	V_y (kN)	V_m (kN)	U_y (cm)	U_m (cm)	U_p (cm)
MW1	1.775	43	95	143	3.06	4.67	8.40
MW2	2.045				2.32	5.81	

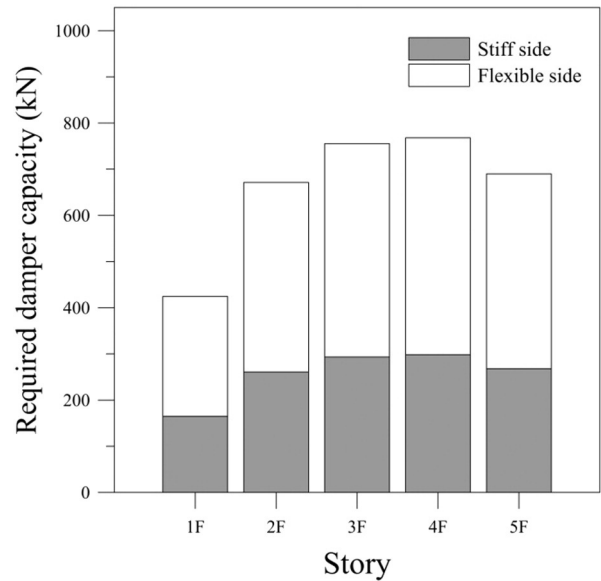


Fig. 18. Required damper capacity at each side of the 5-story model structure.

ductility demands of the model structures retrofitted with the slit dampers obtained from the time history analyses using the seven artificial earthquake records are depicted in Fig. 13. It can be observed that in all model structures the mean ductility demands are less than the given limit state of 3.0 after retrofit. As in the previous case the mean ductility demands on the stiff and the flexible sides coincide quite well with each other. For a slit plate damper composed of nine strips with width (b) of 2 cm, thickness (t) of 2 cm, and length (l_o) of 20 cm, the yield force and yield displacement are computed to be 146 kN and 0.225 cm considering the overstrength factor of 1.5. This particular damper can be used at the flexible side of the model C which requires a slit damper with a yield force of 141.2 kN as can be observed in Table 1. When the maximum story drift of 1.5% of the story height occurs in the model structure, which is 4.5 cm, the maximum ductility ratio of the slit damper is 20. Chan and Albermani [15] carried out an experimental study of steel slit dampers and showed that a ductility ratio over 55 could be achieved in the slit dampers. As the maximum displacements of the model structures retrofitted

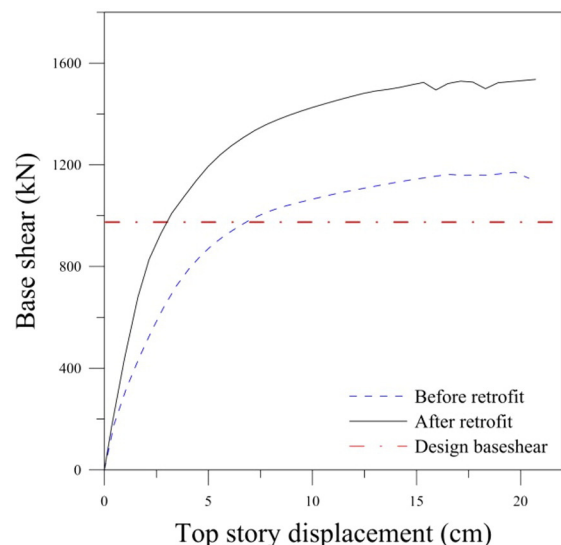


Fig. 19. Pushover curves at CM of the 5-story structure before and after retrofit.

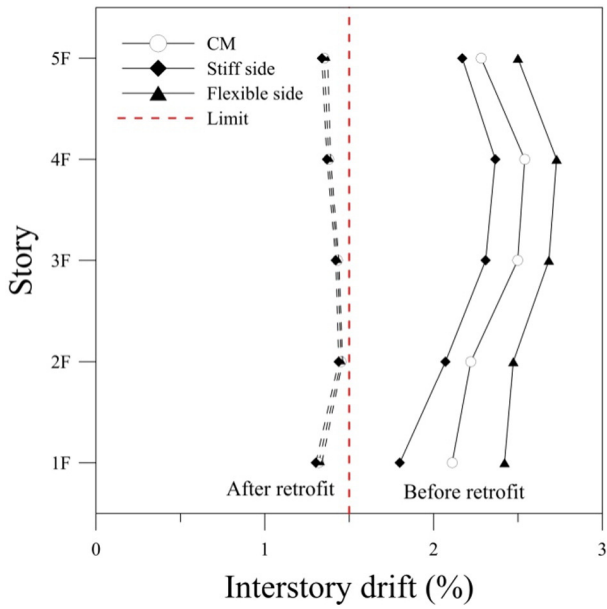


Fig. 20. Mean maximum inter-story drift ratio of the 5-story structure before and after retrofit.

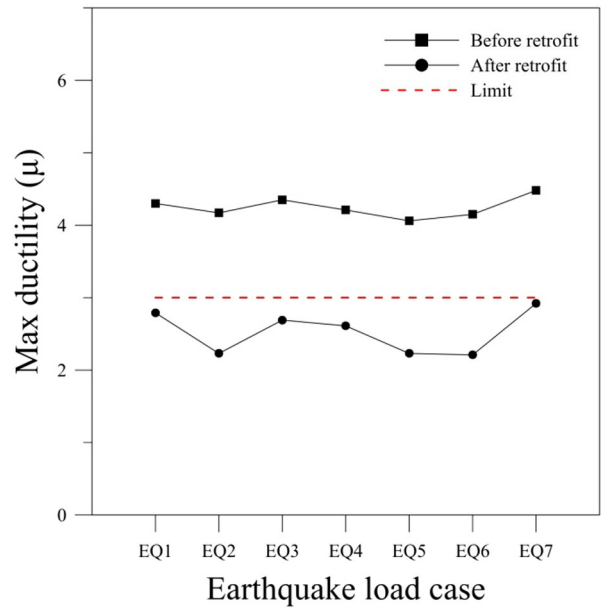


Fig. 22. Mean maximum ductility demands of the 5-story structure before and after retrofit.

with the slit dampers are within 1.5% of the story height, the maximum ductility of the slit damper is well within the limit state.

5. Seismic retrofit of low-rise asymmetric structures

5.1. Modeling of masonry walls

The multi-story structures considered in this study are typical low-rise multi-unit residential buildings in Korea which consist of reinforced concrete moment frames and shear walls. In those structures partition walls or exterior surfaces are constructed with masonry walls which are generally neglected in structural analysis. It has been reported, however, that in low-rise RC structures the masonry walls may affect the seismic performance of the structures significantly [20].

The contribution of masonry walls may be more significant when the asymmetry is enhanced by the uneven distribution of masonry walls.

In this study masonry walls were replaced by equivalent struts following the procedure recommended in FEMA 356 [12] in seismic performance evaluation of the model structures. Fig. 14 shows the configuration of equivalent strut, where H_c is the height of the columns, H_m and L_m are the height and length of the masonry wall, r_m is the length of the strut, and W_{eff} is the effective width of the strut which is computed using the following equation:

$$W_{eff} = 0.175 (\lambda H_m)^{-0.4} \sqrt{H_m^2 + L_m^2}; \quad \lambda = \sqrt[4]{\frac{E_w t \sin 2\theta}{4E_c I_c H_c}} \quad (20)$$

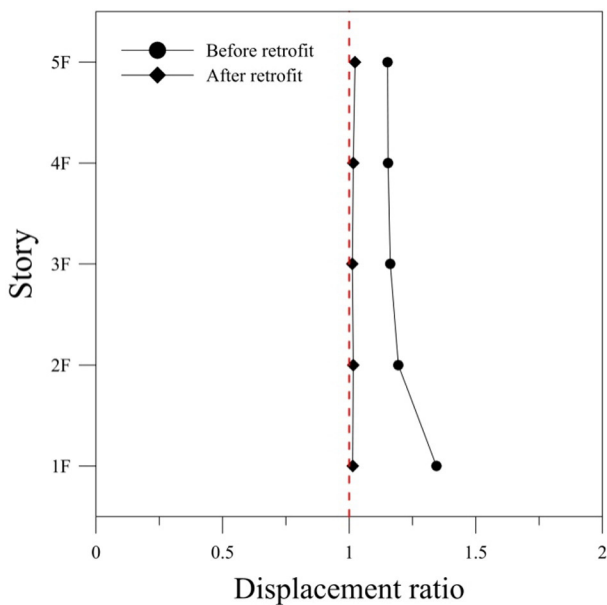


Fig. 21. Ratio of maximum story displacements at flexible and stiff sides of the 5-story structure.

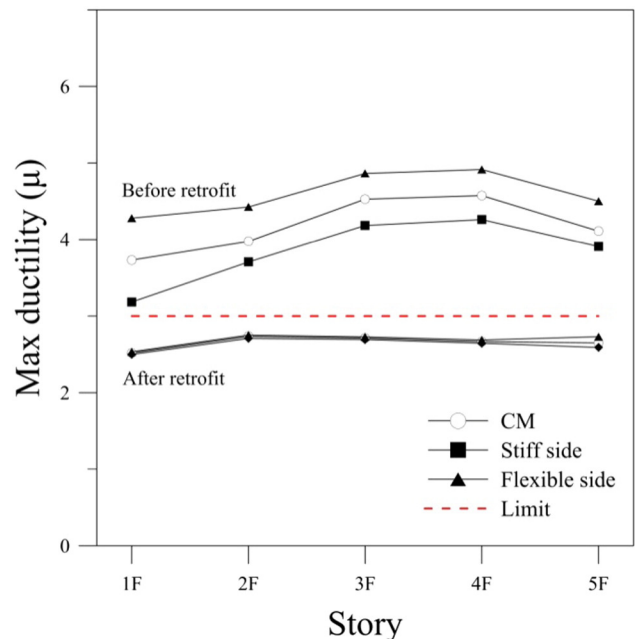


Fig. 23. Mean maximum ductility demands at each story of the 5-story structure.



Fig. 24. Perspective view of the 4-story structure with plan and vertical asymmetry.

where E_w and E_c are the elastic modulus of masonry walls and columns, respectively, t is the thickness of the wall, θ is the slope of the strut, I_c is the moment of inertia of columns, and H_c is the height of columns. Fig. 15 shows the nonlinear modeling of the force–displacement relationship of masonry walls presented in Madan et al. [21]. The strength and displacement factors which define the nonlinear envelop curve are obtained as follows

$$V_p = 0.3V_m, U_p = 3.5(0.01h_m - U_m), \alpha = 0.2 \quad (21)$$

where V_m is the maximum shear strength, V_p is the post-peak residual shear strength, U_m and U_p are the corresponding displacements, and α is the post-yield stiffness.

5.2. Five-story structure with plan asymmetry

In this section the proposed seismic retrofit scheme was applied to a five story reinforced concrete moment frame with eccentrically located core wall. Fig. 16 shows the perspective view of the model structure with plan eccentricity. The story height of the structure is 2.9 m, and the structural plan is shown in Fig. 17. The locations of the masonry walls are indicated in gray color. The structure was designed using the dead and live loads of 5 and 2 kN/m², respectively, and the wind load with a basic wind speed of 30 m/s. Seismic load was not considered in the structural design assuming that the structure was designed before the seismic design code was established. The first three natural periods of the structure were computed as follows: (i) $T_1 = 0.31$ s along the x (longitudinal) direction, (ii) $T_2 = 0.25$ s along the y (transverse) direction, and (iii) $T_3 = 0.20$ s along the z (rotational) directions. Tables 2 and 3 show the design parameters and the nonlinear modeling coefficients for the effective struts used in the modeling of the 5-story model structure with plan irregularity. The shear and the compressive strengths of the masonry walls were obtained from the Korea Building Code [28]. In an irregularly asymmetric multi-story structure, it is not so obvious to locate the center of rigidity, CR, as in a regularly asymmetric structure. Readers are referred to the previous studies [22–26] for calculation of the torsional stiffness radius of multi-story or irregularly asymmetric structures. In this study the center of mass and the center of rigidity of the model structure were obtained using the structural analysis and design program package MIDAS GenW [27] which was also used to design the model structure. In this structure the eccentricity, the distance between the CR and CM, was estimated to be 33.4% of the width of the structure. The locations of the center of mass (CM) and the center of rigidity (CR) are shown in the structural plan. The first three natural periods of the structure were computed

as follows: (i) $T_1 = 0.38$ s along the y (transverse) direction and (ii) $T_2 = T_3 = 0.27$ s along the x (longitudinal) and z (rotational) directions.

As the structure was not designed for seismic load, the purpose of this study was to retrofit the structure in such a way that the ductility demand at the CM of the system at the top story was within the given ductility limit state of 3.0 when it is subjected to the design seismic load. The design seismic load used for the retrofit design was determined from the design spectrum specified in the ASCE 7-13 [1] constructed using the seismic ground acceleration coefficients, S_{D5} and S_{D1} , of 0.49 and 0.28, respectively. Nonlinear dynamic analyses were carried out using the seven artificial records to obtain the maximum roof displacement of the model structure. Pushover analysis of the model structure was also carried out using the lateral load proportional to the fundamental mode shape of the structures until the maximum displacement at CM reached 5% of the total height. The yield displacement was obtained by idealizing the pushover curves as recommended in the ASCE/SEI 41 [17]. The first line segment of the idealized force–displacement has a slope equal to the effective lateral stiffness, which is taken as the secant stiffness calculated at a base shear force equal to 60% of the effective yield strength of the structure. The second line segment represents the positive post-yield slope, determined by the point of maximum base shear and a point at the intersection with the first line segment such that the areas above and below the actual curve are approximately balanced. The third line segment representing the negative post-yield slope is determined by the point at the end of the positive post-yield slope and the point at which the base shear degrades to 60% of the effective yield strength. Then the system ductility demand was computed by dividing the maximum displacements at CM with the yield displacement obtained from pushover analysis. The mean value of the seven system ductility demands was used to evaluate the total required damping for seismic retrofit, which was distributed throughout the stories based on the relative story ductility demands. Then the equivalent damping assigned for each story was distributed to the stiff and the flexible sides based on their relative ductility demands.

Fig. 18 shows the computed slit damper capacity required for each story and each side of the model structure. It can be observed that the largest amount of damper capacity is required at the 3rd and 4th stories and the smallest capacity is required at the first story. It also can be noticed that relatively larger amount of damper capacity is required for the flexible side, and the distribution ratios are similar throughout the stories. The steel plate slit dampers were designed using the required damper capacity and were installed at each side of the model structure at the locations marked in the structural plan.

Fig. 19 shows the pushover curves of the model structure at CM before and after retrofit, where it was observed that as a result of the seismic retrofit the overall strength increased by about 35%. Fig. 20 shows the mean maximum inter-story drift ratio at CM, flexible side, and stiff side before and after retrofit obtained using the seven artificial records scaled to fit the design spectrum of the model structure. It can be observed that before retrofit the inter-story drift at each story and at each side exceeded 1.5% of the story height which is considered to be the limit state for the design seismic load. However after installation of the slit dampers designed following the proposed procedure, the inter-story drifts at all locations decreased below the limit state. Fig. 21 depicts the ratio of the maximum story displacements at flexible and stiff sides before and after retrofit, where it can be observed that as a result of seismic retrofit using the slit dampers, the displacement at the flexible and the stiff sides became almost identical.

Fig. 22 depicts the maximum ductility demands at the CM of the top story before and after the retrofit computed using the seven artificial earthquake records. It can be observed that before the retrofit the ductility demands for all earthquake records are larger than 4.0, whereas the values fall within 2.0 to 3.0 after the retrofit. Fig. 23 shows the mean maximum ductility demands at each story of the 5-story structure, where it can be observed that after the retrofit the ductility demands at all stories decreased below 3.0 and that those at all sides became almost

identical except at the top story. In addition the ductility demands at all stories became more uniformly distributed after the retrofit.

5.3. Four-story structure with plan and vertical asymmetries

The analysis model structure is a four story RC structure with parking spaces in the first story and residential spaces in the second to fourth stories. The structure consists of moment frames and core walls in the first story and of only shear walls above that level, which leads to vertically irregular building. The core walls are located eccentrically resulting in plan asymmetry. Figs. 24 and 25 depict the perspective view and the structural plan of the 4-story structure, respectively. The story height is 2.6 m in all stories. The overall eccentricity perpendicular to the loading direction was evaluated to be 20.3% of the overall building width. The first three natural periods are 0.23 s (longitudinal), 0.16 s (rotational), and 0.11 s (transverse).

To carry out the retrofit design in such a way that the ductility demand at the CM of the system at the top story is within the given ductility limit state of 3.0, nonlinear dynamic analyses were carried

out first with the seven artificial earthquake records to obtain the mean maximum roof displacements at CM of the model structure. Then the system ductility demand was computed and was turned into required damping using Eq. (14), which was distributed to each story and to each side based on the relative story ductility demands. The required damping at each side was transformed into the required yield strength of slit dampers using Eq. (15).

Fig. 26 shows the computed slit damper capacity required for each story and each side of the model structure. It can be observed that the significant amount of damper capacity is allocated to the flexible side in the first story. The slit dampers were designed using the required damper capacity and were installed at each side of the model structure at the locations marked in the structural plan.

Fig. 27 depicts the pushover curves of the model structure before and after retrofit, where it was observed that as a result of the seismic retrofit the overall strength increases by about 11%. Fig. 28 shows the mean maximum inter-story drift ratio of the structure at each story before and after retrofit averaged over the seven time history analysis results. It can be observed that before retrofit the inter-story drift is

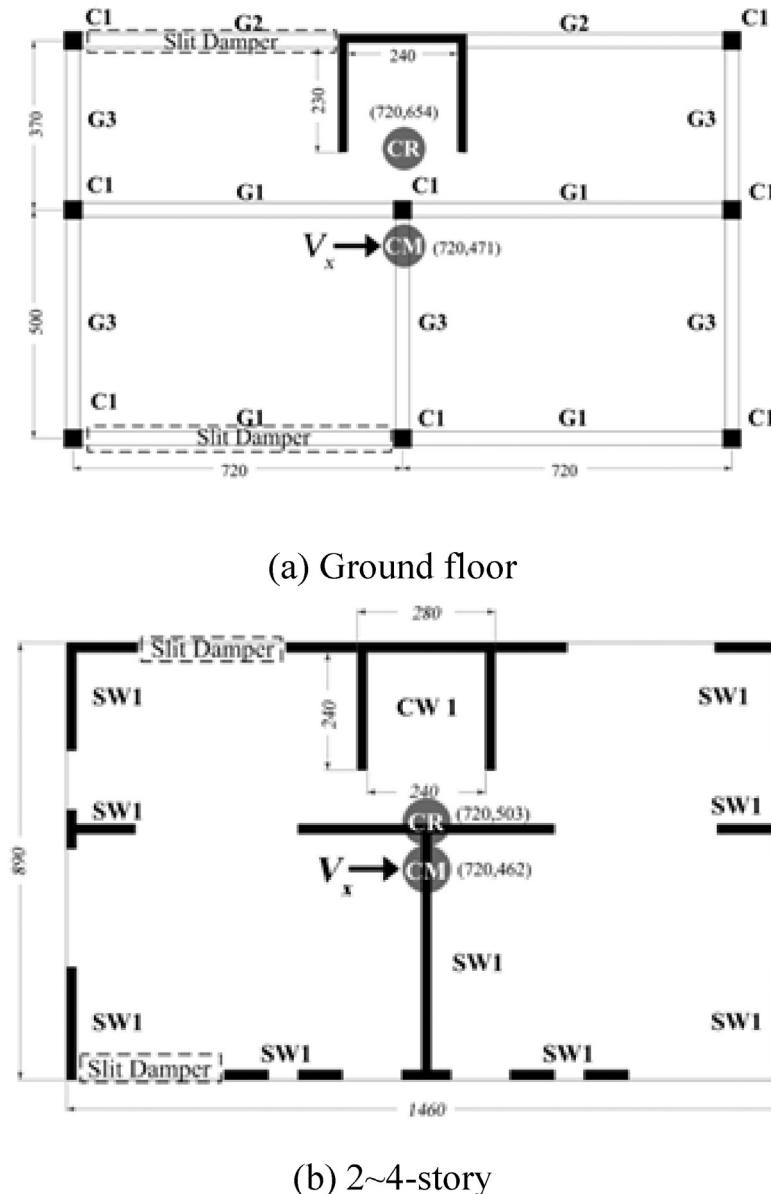


Fig. 25. Structural plan of the 4-story structure.

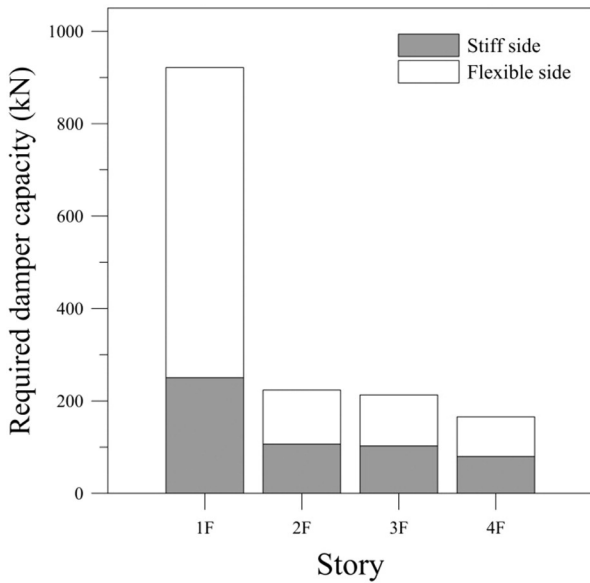


Fig. 26. Required damper capacity of the 4-story structure.

the most significant at the first story which is the soft story. After installation of the slit dampers designed following the proposed procedure, the inter-story drifts at all locations decrease below 1.5% of the story height and became uniformly distributed. Fig. 29 depicts the ratio of the maximum story displacements at the flexible and stiff sides at each story before and after retrofit, where it can be observed that after the retrofit, the displacements at the flexible and the stiff sides become almost identical except for the slight difference in the first story.

Fig. 30 depicts the maximum ductility demands at the top story CM of the structure before and after the retrofit computed using the seven artificial earthquake records. It can be observed that before the retrofit the ductility demands for all earthquake records are larger than 3.5, whereas in most cases they decrease below 3.0 after the retrofit using the slit dampers.

6. Conclusion

Steel plate slit dampers are considered as efficient damping devices for seismic retrofit of existing structures with high energy dissipation

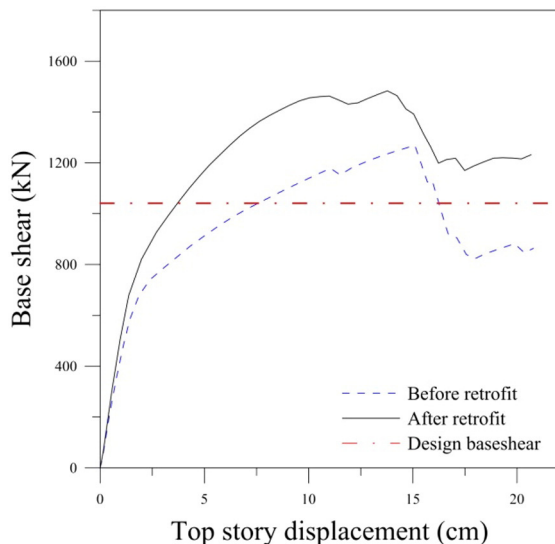


Fig. 27. Pushover curves of the 4-story structure before and after retrofit.

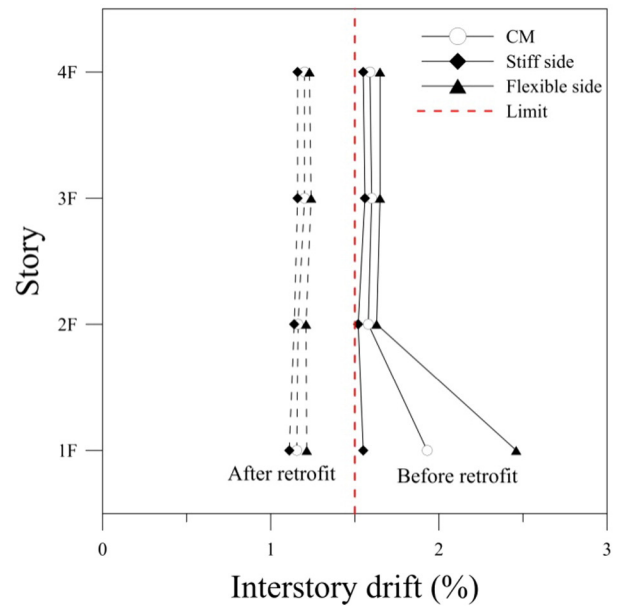


Fig. 28. Mean maximum inter-story drift ratios of the 4-story structure before and after retrofit.

capability and relatively low manufacturing cost. In this study a systematic seismic retrofit design procedure was developed for determining proper amount of steel plate slit dampers required to restrain the seismic response of low-rise asymmetric structures within a given target performance level. The main idea of the retrofit method is to install slit dampers in such a way that the ductility demands at both stiff and flexible edges are limited within a given target value. The procedure was applied to seismic retrofit of single-story idealized asymmetric structure, five-story plan-wise asymmetric structure, and a four-story structure with plan and vertical asymmetry subjected to earthquake loads.

According to the nonlinear analysis results, the asymmetric structures retrofitted with the steel plate slit dampers installed in accordance with the proposed procedure showed satisfactory performance in both the stiff and the flexible edges. It was observed that after the seismic

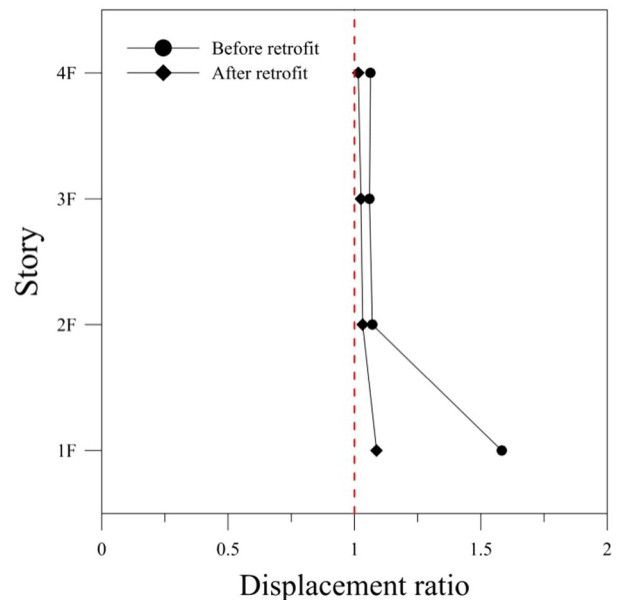


Fig. 29. Ratios of maximum story displacements at flexible and stiff sides of the 4-story structure.

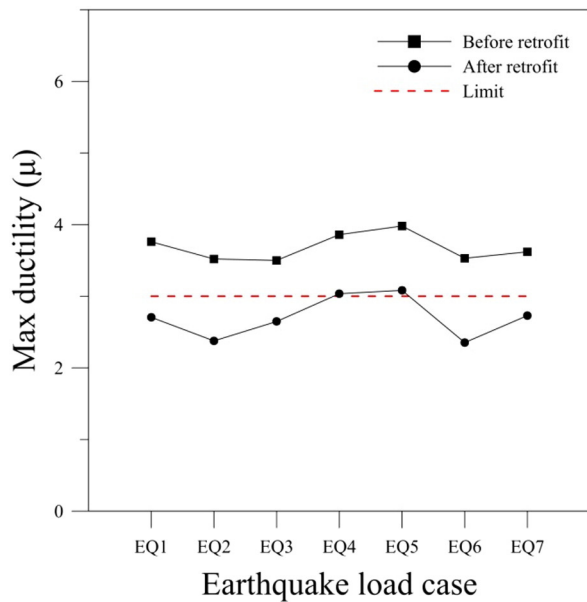


Fig. 30. Mean maximum ductility demands of the 4-story structure before and after retrofit.

retrofit the inter-story displacements and the ductility demands were reduced below the desired limit states, and those at the flexible and the stiff sides became almost identical. Based on these observations it was concluded that the design method for steel plate slit dampers based on the ductility demand was effective in seismic retrofit of asymmetric structures.

Acknowledgment

This research was supported by a grant (13AUDP-B066083-01) from Architecture & Urban Development Research Program funded by Ministry of Land, Infrastructure and Transport of Korean government.

References

- [1] ASCE, Minimum Design Loads for Buildings and Other Structures, ASCE Standard ASCE/SEI 7-13, American Society of Civil Engineers, Reston, Virginia, 2013.
- [2] R.K. Goel, Effects of supplemental viscous damping on seismic response of asymmetric-plan systems, *Earthq. Eng. Struct. Dyn.* 27 (2) (1998) 25–141.

- [3] J. Kim, S. Bang, Optimum distribution of added viscoelastic dampers for mitigation of torsional responses of plan-wise asymmetric structures, *Eng. Struct.* 24 (10) (2002) 1257–1269.
- [4] W.H. Lin, A.K. Chopra, Understanding and predicting effects of supplemental viscous damping on seismic response of asymmetric one-story systems, *Earthq. Eng. Struct. Dyn.* 30 (10) (2001) 1475–1494.
- [5] J.C. De La Llera, J.L. Almazan, I. Vial, V. Ceballos, M. Garcia, Analytical and experimental response of asymmetric structures with friction and viscoelastic dampers, 13th World Conference on Earthquake Engineering, Vancouver, B.C., Canada, 2004.
- [6] L. Petti, M. De Luliis, Torsional seismic response control of asymmetric-plan systems by using viscous dampers, *Eng. Struct.* 30 (11) (2008) 3377–3388.
- [7] S.V. Mevada, R.S. Jangid, Seismic response of asymmetric systems with linear and non-linear viscous dampers, *Int. J. Adv. Struct. Eng.* 4 (5) (2012) 1–20.
- [8] S.N. Khante, B.P. Nirwan, Mitigation of response of asymmetric building using passive tuned mass damper, *Int. J. Sci. Eng. Res.* 4 (7) (2013) 1721–1727.
- [9] S.D. Bharti, S.M. Dumne, M.K. Shrimali, Earthquake response of asymmetric building with MR damper, *Earthq. Eng. Vib.* 13 (2) (2014) 305–316.
- [10] J.L. Almazana, J. Espinozab, J.J. Aguirrea, Torsional balance of asymmetric structures by means of tuned mass dampers, *Eng. Struct.* 42 (2012) 308–328.
- [11] T. Paulay, Torsional mechanisms in ductile building system, *Earthq. Eng. Struct. Dyn.* 27 (10) (1998) 1101–1121.
- [12] FEMA, Prestandard and Commentary for the Seismic Rehabilitation of Buildings, FEMA 356, Federal Emergency Management Agency, Washington, D.C., 2003
- [13] SEAOC, Performance-based Seismic Engineering, Vision 2000, Structural Engineers Association of California, Sacramento, CA, 1995.
- [14] ASCE, Seismic Rehabilitation of Existing Buildings, ASCE Standard ASCE/SEI 41-13, American Society of Civil Engineers, Reston, Virginia, 2013.
- [15] R.W.K. Chan, F. Albermani, Experimental study of steel slit damper for passive energy dissipation, *Eng. Struct.* 30 (4) (2008) 1058–1066.
- [16] Perform 3D, Nonlinear Analysis and Performance Assessment for 3D Structures—User Guide, Computers & Structures, Inc., Berkeley, CA, 2006.
- [17] T. Paulay, M.J.N. Priestley, Seismic Design of Reinforced Concrete and Masonry Building, John Wiley & Sons, Inc., 1992
- [18] ASCE, Seismic Evaluation and Retrofit of Existing Buildings. ASCE/SEI 41-13, American Society of Civil Engineers, Virginia, 2010.
- [19] Eqmaker, Open Source Program Software for Generation of Artificial Earthquakes, 2009 (<http://eqmaker.kr>).
- [20] P.M. Pradhan, Equivalent strut width for partial infilled frames, *J. Civ. Eng. Res.* 2 (5) (2012) 42–48.
- [21] A. Madan, A.M. Reinhorn, J.B. Mander, R.E. Valles, Modeling of masonry infill panels for structural analysis, *J. Struct. Eng.* 123 (10) (1997) 1295–1302.
- [22] T. Makarios, A. Anastassiadis, Real and fictitious elastic axes of multi-storey buildings: theory, *Struct. Des. Tall Special Build.* 7 (1) (1998) 33–55.
- [23] T. Makarios, A. Anastassiadis, Real and fictitious elastic axes of multi-storey buildings: applications, *Struct. Des. Tall Special Build.* 7 (1) (1998) 57–71; T. Makarios, Practical calculation of the torsional stiffness radius of multi-storey tall buildings, *Struct. Des. Tall Special Build.* 17 (1) (2008) 39–65.
- [24] E.M. Marino, P.P. Rossi, Exact evaluation of the location of the optimum torsion axis, *Struct. Des. Tall Special Build.* 13 (4) (2004) 277–290.
- [25] A.M. Athanopoulou, T. Makarios, K. Anastassiadis, Earthquake analysis of isotropic asymmetric multistorey buildings, *Struct. Des. Tall Special Build.* 15 (4) (2006) 417–443.
- [26] M. Bosco, E.M. Marino, P.P. Rossi, An analytical method for the evaluation of the in-plan irregularity of non-regularly asymmetric buildings, *Bull. Earthq. Eng.* 11 (5) (2013) 1423–1445.
- [27] M.I.D.A.S. GenW, General Structure Design System for Windows, MIDAS Information Technology Co. Ltd., 2014
- [28] Korea Building Code, Architectural Institute of Korea, Seoul, Korea, 2009.